

# Ca II 8542 Å sunspot oscillations observed with THEMIS\*

K. Tziotziou<sup>1</sup>, G. Tsiropoula<sup>2</sup>, and P. Mein<sup>1</sup>

<sup>1</sup> Observatoire de Paris, Section de Meudon, DASOP, 92195 Meudon Principal Cedex, France  
e-mail: [Kostas.Tziotziou@obspm.fr](mailto:Kostas.Tziotziou@obspm.fr), e-mail: [Pierre.Mein@obspm.fr](mailto:Pierre.Mein@obspm.fr)

<sup>2</sup> National Observatory of Athens, Institute for Space Applications and Remote Sensing, 15236 Palea Penteli, Greece  
e-mail: [georgia@space.noa.gr](mailto:georgia@space.noa.gr)

Received 25 April 2001 / Accepted 7 September 2001

**Abstract.** Oscillations in the umbra and the penumbra of an isolated sunspot located near the solar disk centre were investigated. The observations were obtained with the Multichannel Subtractive Double Pass (MSDP) spectrograph operating in the Ca II 8542 Å line and installed at the focus of THEMIS (Tenerife). From the MSDP data, two-dimensional intensity and Doppler shift images were computed at different wavelengths within the line. Intensity and Doppler shift oscillations in the umbra and the penumbra of the sunspot showing up as umbral flashes and penumbral waves were analyzed using a 23 min time series with a cadence of 46 s. The Ca II umbral flash intensity profile shows an emission core in its blue wing. We investigate the relation between umbral flashes and running penumbral waves by a power spectrum analysis which shows a 6 mHz frequency for the standing umbral oscillations (flashes) which are observed only on the upper half part of the umbra. The running penumbral waves propagate with an average phase velocity of  $16 \text{ km s}^{-1}$  and their frequency is constant in the penumbra and equal to 3 mHz. Although the time slice images suggest that umbral flashes and running penumbral waves are probably due to the same resonator, the power analysis shows no direct relationship between the two phenomena.

**Key words.** Sun: chromosphere – Sun: oscillations – Sun: sunspots

## 1. Introduction

Spots and their surroundings are among the more striking manifestations of activity appearing on the solar atmosphere. Studies of their evolution with time have revealed the existence of many dynamical phenomena associated with them, some of which have an oscillatory nature, like umbral flashes, umbral oscillations and running penumbral waves.

The study of oscillations in the atmosphere of sunspots dates back to the detection of umbral flashes in intensity images of the Ca II H and K lines and the infrared triplet of Ca II by Beckers & Tallant (1969). Three years later, intensity and/or velocity in various spectral lines observations revealed the existence of the 5-min oscillations in the umbral photosphere (Bhatnagar et al. 1972), of the 3-min oscillations in the umbral chromosphere (Beckers & Schultz 1972; Giovanelli 1972) and of the running penumbral waves (Zirin & Stein 1972; Giovanelli 1972). Since then

many observations have been performed at photospheric, chromospheric and transition region levels and increasing theoretical efforts have been undertaken in order to understand these periodic phenomena which contain crucial information regarding the dynamic structure of sunspots (see reviews by Lites 1992; Staude 1998).

The power spectrum of umbral oscillations usually shows sharp peaks which are closely packed and concentrated in different period bands depending on the atmospheric height. At the photospheric level a peak within the 5-min band ( $200 \text{ s} < P < 400 \text{ s}$ ) is predominant with an average rms velocity amplitude of  $75 \text{ m s}^{-1}$  (Lites 1992). At the chromospheric and transition region levels a peak within the 3-min band ( $100 \text{ s} < P < 200 \text{ s}$ ) is mainly observed (Brynildsen et al. 1999). At the chromospheric level typical velocity amplitudes are of the order of  $6 \text{ km s}^{-1}$ , although amplitudes as large as  $8 \text{ km s}^{-1}$  have been derived from Doppler shifts of the H $\alpha$  line (Tsiropoula et al. 2000). Today, it is generally believed that umbral flashes and umbral oscillations are different manifestations of the same phenomenon. Chromospheric umbral oscillations are present in almost every sunspot umbra at all times, whereas umbral flashes occur only locally and occasionally when the velocity amplitudes exceed a value, which, e.g., is  $\sim 5 \text{ km s}^{-1}$  for the Ca II K line. Flashes

*Send offprint requests to:* K. Tziotziou,  
e-mail: [Kostas.Tziotziou@obspm.fr](mailto:Kostas.Tziotziou@obspm.fr)

\* Based on observations made with the THEMIS telescope operated on the island of Tenerife by CNRS-CNR in the Spanish Observatorio del Teide of the Instituto de Astrofísica de Canarias.

in H $\alpha$  are more rarely observed and may require a higher velocity amplitude.

Different oscillation patterns have been reported inside the umbra due to its inhomogeneous nature. For instance, Abdelatif et al. (1986) demonstrated that coherently oscillating elements with 5-min periods appear to cover a large fraction of the umbral area. Lites (1986), on the other hand, claimed that the umbra at the chromospheric level does not oscillate as a whole, but that the oscillations occur in small spatial regions within the umbra, the “oscillating elements”, with sizes of 3''–4''.

Recently Socas-Navarro et al. (2000a, 2000b) observed that for the Ca II infrared triplet lines there is a periodic occurrence of anomalous, asymmetric circular polarization profiles in the umbral chromosphere. They have associated it with umbral flashes and found a periodicity of  $\sim 150$  s. Moreover, López Ariste et al. (2001) have shown that umbral flashes, observed in the Ca II infrared triplet lines with THEMIS, have linear polarization signals delayed in time and shifted in space when compared with the corresponding circular polarization signals. They have suggested that flashes are produced by a perturbation propagating along the magnetic field lines bending out towards the penumbra.

Running penumbral (RP) waves show a characteristic pattern of alternating dark and bright bands in velocity images. They start out as arcs surrounding the umbra and having azimuthal extents of 90°–180° and sometimes even 360°. They have periods of 180–300 s and radial extents 2300–3800 km and they propagate more or less uniformly outwards, becoming gradually invisible when or before they reach the outer boundary of the penumbra. RP waves are closely related to umbral oscillations. Tsiropoula et al. (1996, 2000) and Alissandrakis et al. (1998) provide clear evidence of waves originating from oscillating elements inside the umbra and propagating through the penumbra. They also found that the propagation speed of the waves decreases from the inner to the outer penumbra. They found phase velocities of the order of 20–30 km s<sup>-1</sup> in the inner penumbra, while in the outer penumbra they measured values between 10 and 16 km s<sup>-1</sup>. Their findings provided a clear evidence that these two phenomena, considered as unrelated in the past, are due to the same physical mechanism.

The aim of this work is to analyze high temporal and spatial resolution MSDP observations in the Ca II 8542 Å line obtained with THEMIS. We investigate intensity and Doppler shift oscillations in the umbra and the penumbra in order to provide further information on the subject of sunspot oscillations.

## 2. Observations and data reduction

The sunspot region NOAA 9131, located near the solar disk centre (N16 W21), was observed on August 21, 2000. The observations were obtained with the MSDP spectrograph (Mein 1991, 1995, 2002) installed at the focus

of THEMIS in Tenerife (Canary Islands) during a six-day observing campaign. Observations in two lines, the Na D<sub>2</sub> 5890 Å and the infrared Ca II 8542 Å were carried out. A two-dimensional field-of-view with good spatial and temporal resolution was recorded simultaneously in 16 channels on a 1536×1024 pixel CCD camera which has a spatial resolution of 0.18''. This permits the reconstruction of the Ca II 8542 Å line profile at every pixel of the field-of-view. All four Stokes parameters were computed for Na D<sub>2</sub> and only Stokes parameters *I* and *V* were computed for Ca II. The use of a grid for slice selections of the field of view in THEMIS (Semel 1980) means that partial adjacent fields of view with a small overlap are used in order to reconstruct the desired field of view. Flat field and dark current corrections were also applied in the observations.

The duration of the Ca II observations, used for the current study, was about 23 min. From 08:32:11 to 08:54:58 UT nine adjacent elementary fields of view were recorded every 46 s, each with an exposure time of 600 ms. These were later combined into a larger field of view containing the sunspot and its surroundings by two-dimensional cross-correlation techniques. The time series consists of a sequence of 30 frames. Intensity at line center,  $\pm 0.12$  Å and  $\pm 0.24$  Å and Doppler shifts – from the shifts of the Ca II profiles relative to the average intensity profile (see Sect. 3) – at  $\pm 0.12$  Å and  $\pm 0.24$  Å were computed by the bisector method. The average profiles of intensity and Doppler shifts were also computed at each pixel by averaging over the entire time sequence. Due to the influence of seeing the spatial resolution reached for these observations is  $\sim 0.5''$ .

The Na D<sub>2</sub> observations, obtained from 09:24:29 to 09:40:23 UT, were used for the construction of the corresponding magnetograms. Two scans of thirty six adjacent fields of view with an exposure time of 300 ms were combined to form two consecutive magnetograms of a large field of view around the aforementioned sunspot. However, due to their low quality (bad seeing), not much detailed information could be extracted from these computed magnetograms.

The observed sunspot was isolated and almost circularly symmetric. However, since we were interested in studying short-period phenomena within our temporal sequence and since we had roughly a 5 s acquisition time for each of the nine composite images of the sunspot in Ca II, a small fraction of the sunspot was not covered (see Fig. 3). As it was measured in intensity images taken at the wings of the Ca II profile, where the intensity contrast between the umbra and the penumbra is larger, the umbra-penumbra boundary is at  $\sim 6''$  from the sunspot center, while the penumbra-superpenumbra boundary is at  $\sim 12.6''$ .

## 3. The Ca II umbral flash profile

When line profiles are available, oscillatory motions in sunspots are usually measured as Doppler shifts of spectral

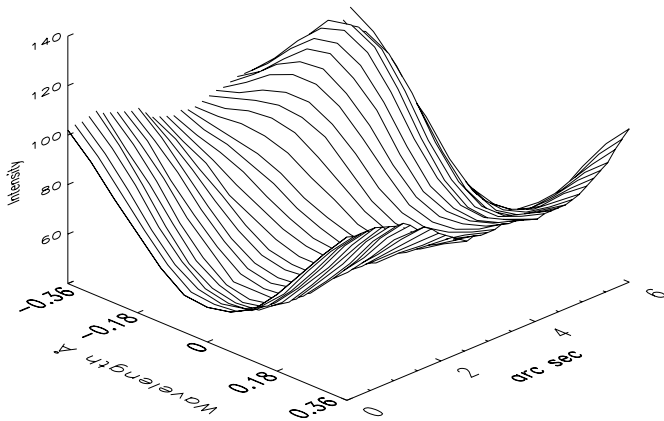


**Fig. 1.** The Ca II 8542 Å profiles along a horizontal cut through an umbral flash showing a strong emission in the blue wing of the profile core where the flash occurs. The wavelength zero is not precise for all profiles but rather indicative.

lines. In this context, absorption lines like  $H\alpha$ , provide important clues about the oscillatory motions, as their intensity fluctuations relative to a mean background can be interpreted as Doppler shift fluctuations.

However, the Ca II 8542 Å line shows an emission on the blue side of its profile during umbral flashes. The correlation of the intensity fluctuations with Doppler shifts is rather problematic in this line and more sophisticated methods based on radiative transfer calculations are needed for the exact computation of the line-of-sight velocity.

In Fig. 1 we show the Ca II 8542 Å profiles along a 6'' horizontal cut through an umbral flash where an emission peak on the blue side of the profile is evident. This has already been documented in the past by several authors (e.g. Kneer et al. 1981; Uexküll et al. 1983). It could be interpreted as a Doppler shift caused by the upward movement of hot material, however, as we have already mentioned, a full model for Ca II profiles in sunspot umbrae should be used in order to calculate the precise velocity.

Figure 1 shows that when – and only when – an umbral flash occurs, which is the observational signature of sunspot material movement, the profiles show both a blueshifted emission core and a redshifted absorption core. The reference wavelength for these shifts is computed from the average Ca II profile of our image. It is the Doppler shifts of the absorption core, computed by the bisector method, that we use for this study. However, in umbral flashes, high redshifts of the absorption core which simply occur due to the presence of the blueshifted emission peak in reality obviously correspond to upward velocities associated with this emission peak. This can be clearly seen in Fig. 2 where we show the Doppler shift along a horizontal cut through an umbral flash, calculated only from the absorption core of the profile (solid line) and from the most prominent core – absorption or emission – of the profile (dotted line) during the umbral flash. In the umbral flash region the most prominent core is the blueshifted emission one, while away from the umbral flash region, where the

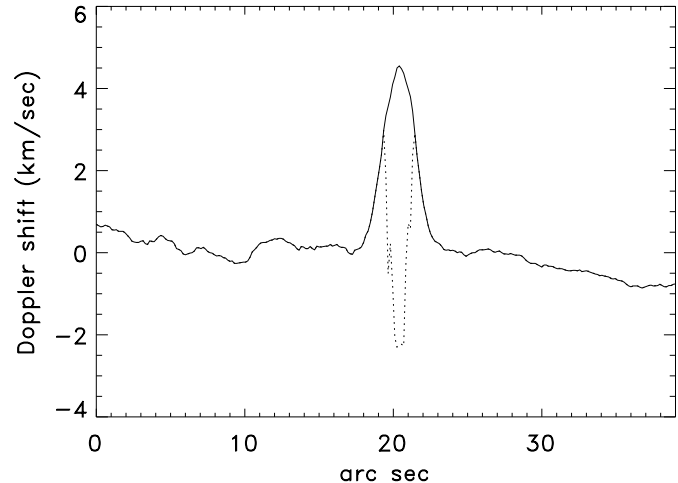


**Fig. 2.** The Doppler shift along a horizontal cut through an umbral flash computed only from the absorption core of the profile (solid line) and from the most prominent core – absorption or emission – of the profile (dotted line) during the umbral flash. In the umbral flash region, high redshifts (positive Doppler shifts) of the absorption core in reality correspond to high upward velocities (negative Doppler shifts) associated with the blueshifted emission core (see text).

Ca II profile shows no emission (see Fig. 1), both Doppler shift calculations obviously coincide.

We always use for this study the computed Doppler shifts with the bisector method of the absorption core of the profile because it is a continuous smooth function, unlike the ones calculated from the most prominent core which, as Fig. 2 shows, have a sudden jump from downwards (positive) to upward (negative) Doppler shifts in the umbral flash region. These Doppler shifts may fail to give a quantitative representation of the actual line-of-sight velocity but they can be used for a qualitative study of sunspot oscillations.

A trace of the Evershed effect is suggested in Fig. 2, with the Doppler shifts being redward on the left side of the cut and blueward on its right side. However, since the correlation of these Doppler shifts with the actual velocity is not known, no quantitative study of the effect can be made.

## 4. Results

In Fig. 3 a sequence of five frames, representing a time series of  $\sim 3.8$  min, of the intensity at line centre and the intensity and Doppler shift at  $\pm 0.12$  Å and  $\pm 0.24$  Å is shown. In the umbra of the sunspot there is a clear indication of periodic brightenings, the well-known umbral flashes. They can be seen in some intensity images, at the centre of the line and at  $\pm 0.12$  Å and less clearly at  $\pm 0.24$  Å. No waves are visible in the intensity images, either at the umbra or the penumbra of the spot. In the Doppler shift images, both umbral flashes and RP waves can be easily seen. Umbral flashes occupy the half upper part of the spot and appear at three distinct locations.

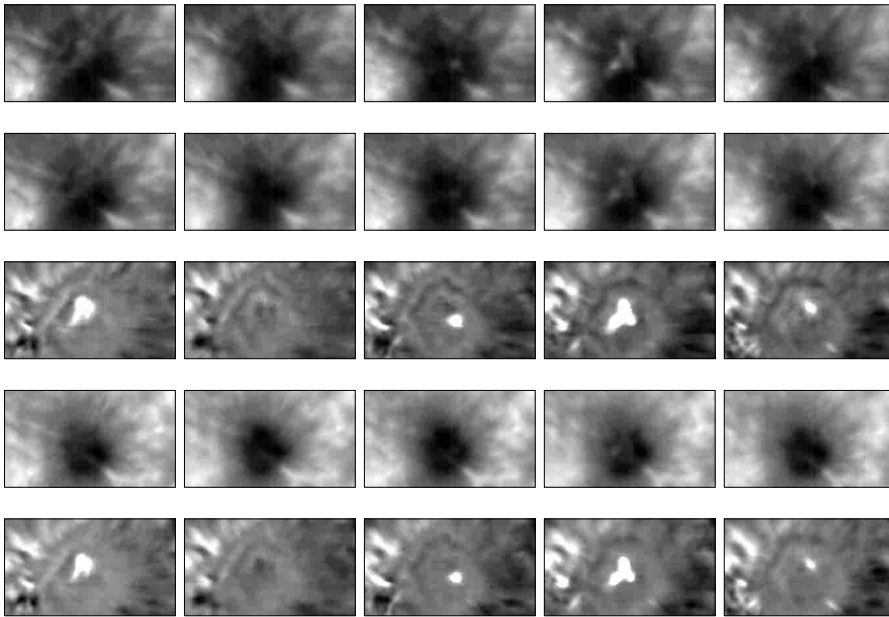


**Fig. 3.** A sequence of five intensity and Doppler shift images of the sunspot observed from 8:45:16 UT with a cadence of 46 s. The field of view is  $39.15'' \times 22.20''$ . The first row gives the intensity at line center, while the other rows give intensity (second and fourth rows) and Doppler shifts (third and fifth rows) at  $\pm 0.12 \text{ \AA}$  and  $\pm 0.24 \text{ \AA}$ . In the Doppler shift images, bright represents redshifts while dark represents blueshifts of the absorption core of the line (see Sect. 3).

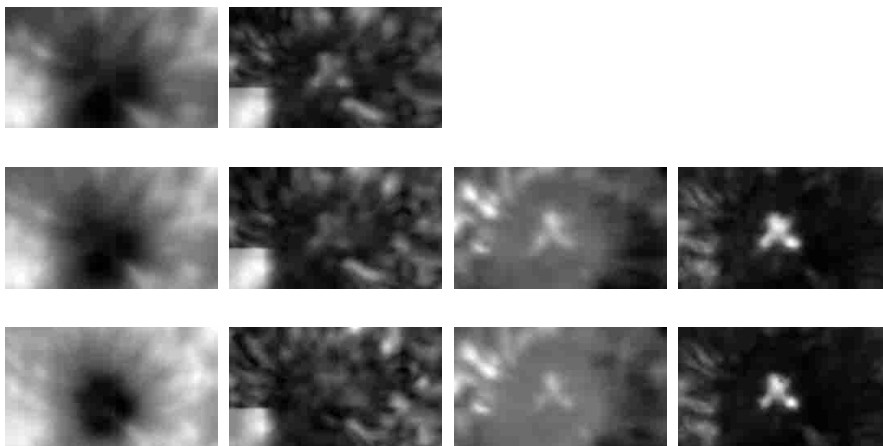


**Fig. 4.** Average (first and third columns) and rms (second and fourth columns) images of intensity at line center (top row) and intensity and Doppler shift at  $\pm 0.12 \text{ \AA}$  (middle row) and  $\pm 0.24 \text{ \AA}$  (bottom row).

Each flash reappears at regular intervals at almost the same location, while the fact that in some images all three flashes are observed and in others only one means that these features oscillate incoherently. From a first look, no proper motion of the umbral flashes towards the edge of the umbra is apparent. The RP waves, which very often have an azimuthal extent of  $250^\circ$ , start at the outer edge of the umbra and propagate through the penumbra (see Fig. 3). At the lower right edge of the spot a bright structure (hereafter BS), reminiscent of a light bridge, can be traced at almost all intensity and Doppler shift images. At this edge no RP waves are observed.

A method very often used in the study of oscillatory phenomena in sunspots is the image subtraction technique (Alissandrakis et al. 1992). This technique, which enhances the fine structure in the umbra and the penumbra and removes the sharp intensity gradient between them, consists of subtracting from each individual image of a time series the “average image” and has been

extensively used for the study of varying phenomena in sunspots (Tsiropoula et al. 2000; Brisken & Zirin 1997; Christopoulou et al. 2000).

In Fig. 4 the average images of Doppler shift and intensity as well as the corresponding rms images for the entire time series are shown. In the time averages of the intensity no clear indication of the umbral flashes or the RP waves is apparent. The bright structure (BS) is obvious in all wavelengths. Rms intensities at line center,  $\pm 0.12 \text{ \AA}$  and  $\pm 0.24 \text{ \AA}$ , as well as average Doppler shifts and rms Doppler shifts at  $\pm 0.12 \text{ \AA}$  and  $\pm 0.24 \text{ \AA}$ , show strong variations at three distinct locations in the upper half of the umbra, apparently associated with the umbral flashes. In the penumbra the observed fluctuations in both the intensity and the Doppler shift images are related to the RP waves.

The influence of seeing on all detected variations is not important since these are usually higher than the reached spatial resolution of  $0.5''$ .

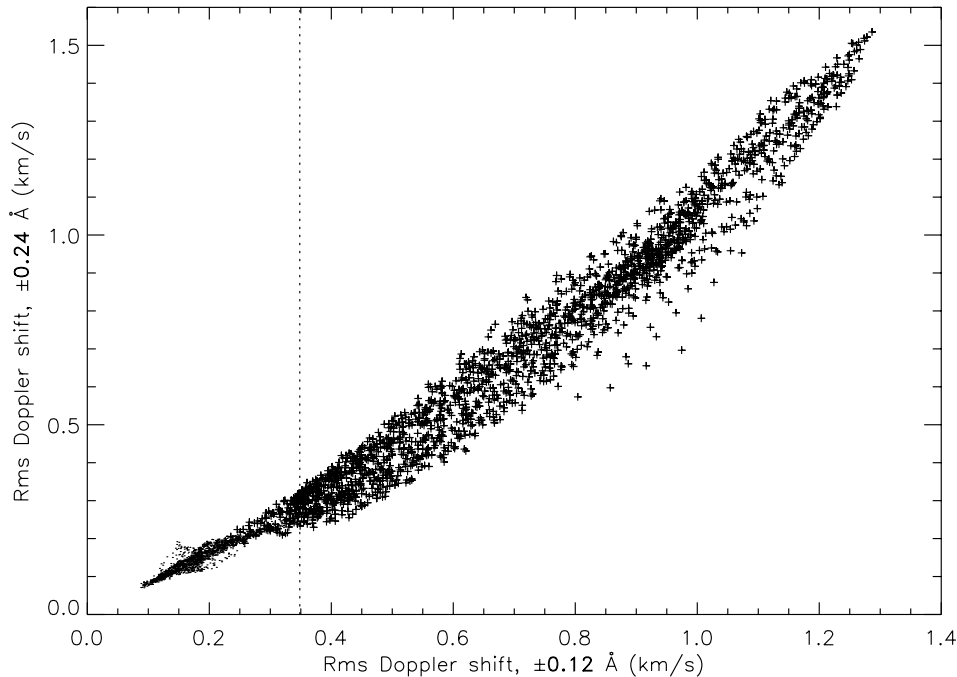


**Fig. 5.** Scatter plot of the rms Doppler shift at  $\pm 0.12$  versus that of  $\pm 0.24$  Å in the umbra of the sunspot. Rms Doppler shifts of the region where umbral flashes occur (see Fig. 6) are shown with plus signs while dots show the dark umbra Doppler shifts. The dashed line represents the maximum rms Doppler shift at  $\pm 0.12$  Å of the dark umbra.

#### 4.1. Umbra and umbral flashes

The scatter plot of the rms Doppler shifts at  $\pm 0.12$  Å and  $\pm 0.24$  Å of the umbra in Fig. 5 shows that Doppler shift fluctuations are very similar. However the plot shows that in the region of the umbra where no umbral flashes are recorded, hereafter called the “dark umbra”, the rms Doppler shifts at  $\pm 0.24$  Å are weaker than their corresponding Doppler shifts at  $\pm 0.12$  Å. Moreover, Doppler shifts in the region of umbral flashes are considerably higher than those of the dark umbra.

The amplitude of the Doppler shifts of umbral flashes is, usually, higher than  $1 \text{ km s}^{-1}$  and, rarely, as high as  $6 \text{ km s}^{-1}$ . In the first row of Fig. 6 we overplot on an intensity image, where the umbra is clearly visible, the contours of Doppler shifts at  $\pm 0.24$  Å of  $4.5$  and  $1.1 \text{ km s}^{-1}$  for all the images of our sequence. These Doppler shift magnitudes are associated with umbral flashes as they are clearly located in the upper half of the spot. Furthermore, umbral flashes have in very rare cases Doppler shifts higher than  $4.5 \text{ km s}^{-1}$ . The contours clearly mark three distinct positions of umbral flashes, already noticed in the rms images (Fig. 4). The total area of umbral flashes at every image of our sequence, with Doppler shifts at  $\pm 0.24$  Å higher than  $4.5$  and  $1.1 \text{ km s}^{-1}$ , is shown in the second row of Fig. 6. The figure suggests that the three umbral flashes never occupy more than 20% of the total area of the umbra which is roughly  $113 \text{ arcsec}^2$ .

As Fig. 6 shows, there are some frames where no umbral flashes are seen. Furthermore, a periodicity in their occurrence is apparent (Fig. 6d). This can be better demonstrated if we take the average intensity and Doppler

shift within the half upper umbra region of Fig. 6, where the umbral flashes occur. In Fig. 7 (solid line) we show the average intensity of the umbral flash region, while in Figs. 8a,b we give the average Doppler shifts of the same region at every image of our time sequence. We also overplot in Fig. 7 the average intensity (dotted line) of the dark lower half sunspot region, where no umbral flashes were recorded, while in Figs. 8c,d we plot the corresponding Doppler shifts. It seems that even the dark umbra has an oscillatory structure. The average intensity of the umbral flash region, which correlates quite well with its corresponding average Doppler shift, verifies our previous observation that umbral flashes are well visible in the intensity images at line center and  $\pm 0.12$  Å, but less visible at  $\pm 0.24$  Å, where the average intensity is almost comparable to that of the dark umbra.

#### 4.2. Running penumbral waves

The RP waves can be very clearly seen in the individual Doppler shift images propagating from the outer edge of the umbra in the penumbra of the sunspot. Two concentric wavefronts, one with positive (away from the observer) and the other with negative Doppler shifts, can usually be detected, although sometimes even 4 wavefronts are visible. In Fig. 9, the Doppler shift variation at  $\pm 0.12$  Å along a horizontal cut through the sunspot center in four consecutive frames beginning at 8:46:47 UT and ending at 8:49:41 UT is shown. A wave is observed traveling through the penumbra with a Doppler shift amplitude  $\sim 0.5 \text{ km s}^{-1}$ . The location of the Doppler shift maximum

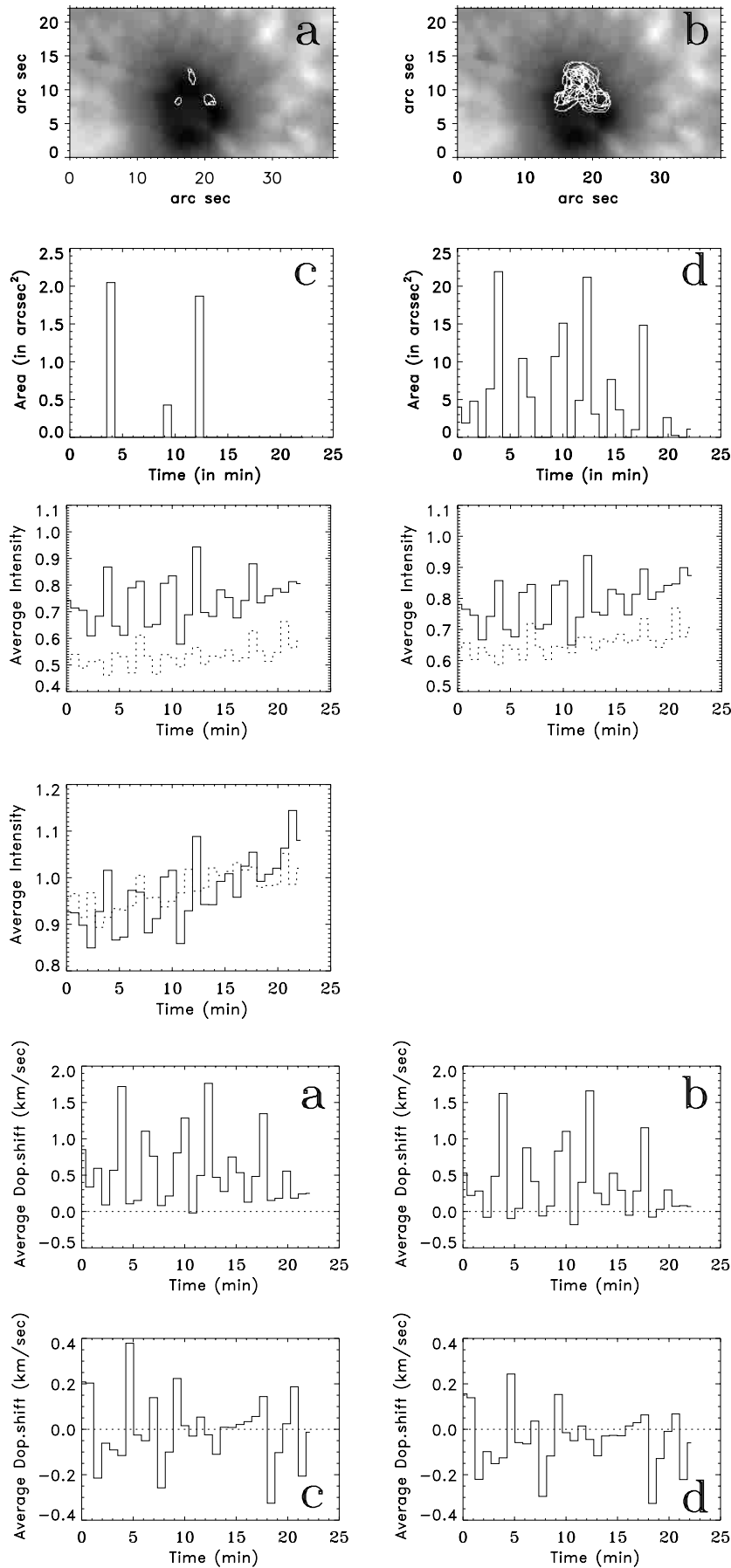


**Fig. 6.** An intensity image at  $\pm 0.24 \text{ \AA}$  (first row) with overimposed Doppler shift contours at  $\pm 0.24 \text{ \AA}$  of **a)**  $4.5 \text{ km s}^{-1}$  and **b)**  $1.1 \text{ km s}^{-1}$  and the total area of umbral flashes per image (second row) when Doppler shifts higher than **c)**  $4.5 \text{ km s}^{-1}$  and **d)**  $1.1 \text{ km s}^{-1}$  are considered.

**Fig. 7.** Average intensity at **a)** line center, **b)**  $\pm 0.12 \text{ \AA}$  and **c)**  $\pm 0.24 \text{ \AA}$  of the upper half umbral region of Fig. 6 where umbral flashes occur (solid line) and the corresponding intensities for the dark lower half umbral region (dotted line). All intensities are normalized to the quiet sun line center intensity.

**Fig. 8.** Average Doppler shifts at **a)**  $\pm 0.12 \text{ \AA}$  and **b)**  $\pm 0.24 \text{ \AA}$  of the upper half sunspot region of Fig. 6 where umbral flashes occur and the corresponding Doppler shifts in **c)** and **d)** for the dark lower half sunspot region.

changes progressively with time, while the Doppler shift amplitude drops as it propagates outward. In the first two images of the plot a flash is also visible in the umbra with a much higher Doppler shift amplitude of  $2 \text{ km s}^{-1}$ . In the third plot this flash almost disappeared, while in the fourth another one appears in a different location within the umbra. From the position of the wave maximum Doppler shift as a function of time we calculate a propagation velocity for the penumbral wave between  $12$  and  $25 \text{ km s}^{-1}$ , with the highest propagation velocity occurring close to the umbra of the spot.

#### 4.3. Time slice images

A better insight into the spatial and temporal characteristics of the umbral flashes and the RP waves can be obtained by making plots of the intensity and Doppler shifts as a function of time, along cuts such as that of Fig. 9. For the intensity plots we use the intensity obtained after applying the subtraction technique described in Sect. 4, hereafter called subtracted intensity. In Fig. 10 we show the subtracted intensity at line center while in Fig. 11 we show the Doppler shifts at  $\pm 0.12 \text{ \AA}$  as a function of position and time along four cuts, in different directions  $45^\circ$  apart, through the sunspot center, starting from the lower outer edge and going clockwise. Umbral flashes are clearly visible in the subtracted intensity and Doppler shift cuts as alternating bright and dark bands almost parallel to the position axis. The intense bright bands of Fig. 11 show high positive (downward) Doppler shifts (redshifts of the absorption core of the Ca II profile) and thus in reality correspond to upward velocities in the umbral flash region as we have already discussed in Sect. 3. The RP waves, which are not observed directly in the intensity images, are visible in the subtracted intensity cuts.

In the Doppler shift cuts they clearly appear as alternating dark and bright diagonal streaks, representing the Doppler shift minima and maxima and curving forward in time. We can always trace back the RP waves inside the umbra, however there are some umbral waves that seem to stop in the umbra-penumbra boundary. It also seems that there are some preferable directions of propagation for the RP waves, with the lower right part of the sunspot region being the least favorite one. There their propagation is clearly affected by the presence of the bright structure (BS). The Na D<sub>2</sub> magnetograms indicate a steeper gradient for the magnetic field towards the left and upper left part of the sunspot which seems to be the preferred direction for the penumbral wave propagation. This implies a coupling of the magnetic field with running penumbral waves, however the lack of a temporal sequence for the Na D<sub>2</sub> line does not permit us to better study the association. The penumbral wave pattern is concave upwards suggesting that the wave propagation velocity decreases from the umbra to the superpenumbra boundary. The average penumbral wave propagation velocity is calculated to be  $16 \text{ km s}^{-1}$ .

#### 4.4. Power spectra of umbral flashes and RP waves

Since a detailed calculation of Ca II profiles is beyond the scope of this paper we cannot perform a frequency analysis at fixed positions within the umbral flash region. However we can study the global behaviour of umbral flashes by performing a power spectrum analysis on the average intensity (Fig. 7, solid line) and Doppler shift (Figs. 8a,b) after subtracting the corresponding mean values. This temporal signal basically corresponds to the average intensity and Doppler shift values of the umbral flash region after applying the subtraction image processing technique we mentioned earlier. After apodization of the time sequence with a cosine bell, in order to diminish the amplitude of artificially induced small frequencies due to the zero padding of our series, we perform a temporal frequency analysis by means of a Fast Fourier Transform. In Fig. 12a we show the resulting power spectra for intensity at line core and at  $\pm 0.12 \text{ \AA}$  and  $\pm 0.24 \text{ \AA}$  and in Fig. 12b the power spectra for Doppler shifts at  $\pm 0.12 \text{ \AA}$  and  $\pm 0.24 \text{ \AA}$ . All power spectra give a frequency for umbral flashes around  $6 \text{ mHz}$  (period of  $167 \text{ s}$ ) which is in accordance with chromospheric umbral oscillations frequency values mentioned previously in literature. We also perform a similar power spectrum analysis for the average intensity (Fig. 7, dotted line) and Doppler shift (Figs. 8c,d) of the dark umbra region. In Fig. 12c we show the resulting power spectra for intensity and in Fig. 12d the power spectra of Doppler shifts. The figures still show a frequency of  $\sim 6 \text{ mHz}$  but they also show several other frequencies including one around  $3 \text{ mHz}$  which is the same, as we will see below, as the frequency of running penumbral waves. High frequency oscillations are concentrated within the dark umbra.

We have performed as well a power spectrum analysis in order to determine the frequency of the waves with distance from the center of the sunspot. We applied the same FFT procedure that we have already described along the same cuts of Fig. 11. Since the resulting power amplitude of umbral flashes would be much higher than the power amplitude of penumbral waves, before applying the FFT procedure we have weighted all Doppler shifts, by the inverse of their rms Doppler shifts in order to enhance the contrast. In Fig. 13 we show the resulting power amplitude as a function of position from the center of the sunspot and frequency. We see that the amplitude is high in the umbral flash region and is associated with oscillations (umbral flashes) which are observed only in the umbra. In the dark umbra region, which is viewed in the top left vertical cut through the center of the sunspot, there are several modes of oscillation, as also Figs. 12c,d suggest. The most prominent mode, which is associated with the running waves, starts out near the outer edge of the umbra and propagates up to the outer edge of the penumbra. However, some power amplitude plots (i.e.  $45^\circ$  cut) suggest that sometimes something affects the propagation of waves in the middle penumbra. Del Toro Iniesta (2001) has suggested that there is a difference in the structure of magnetic fields from the middle penumbra outwards,

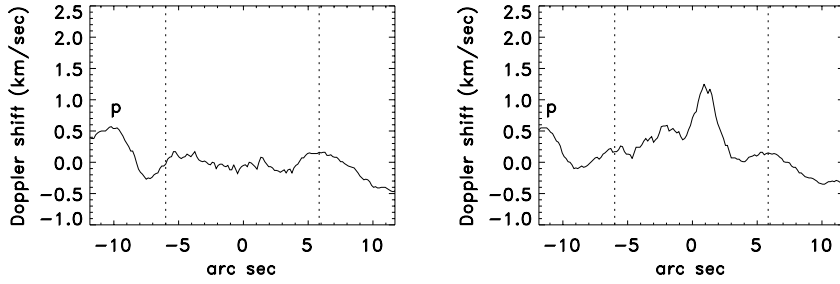
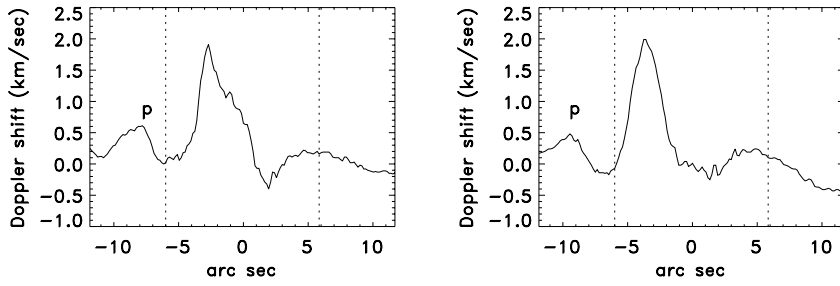


**Fig. 9.** Temporal evolution of the Doppler shift along an horizontal cut through the center of the sunspot from 8:46:47 UT to 8:49:41 UT showing the propagation of a running penumbral wave (p). The dotted lines mark the boundary between the umbra and the penumbra.

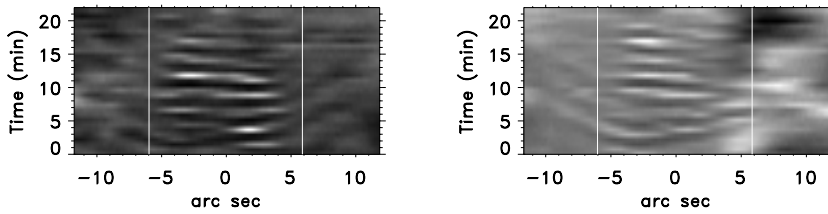
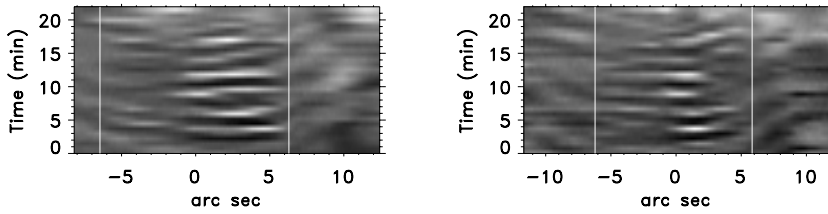


**Fig. 10.** The subtracted intensity (see text) at line center as a function of position and time for four cuts through the center of the sunspot, oriented  $45^\circ$  apart and starting with the vertical one. The bright vertical lines mark the approximate boundary of the umbra.

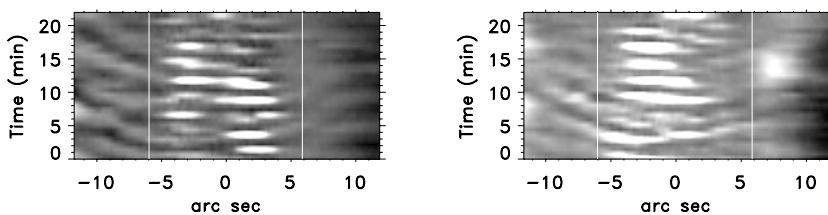
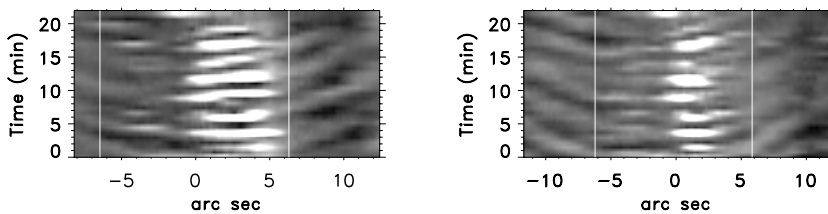


**Fig. 11.** The Doppler shift as a function of position and time for four cuts through the center of the sunspot, oriented  $45^\circ$  apart and starting with the vertical one. The bright vertical lines mark the approximate boundary of the umbra.



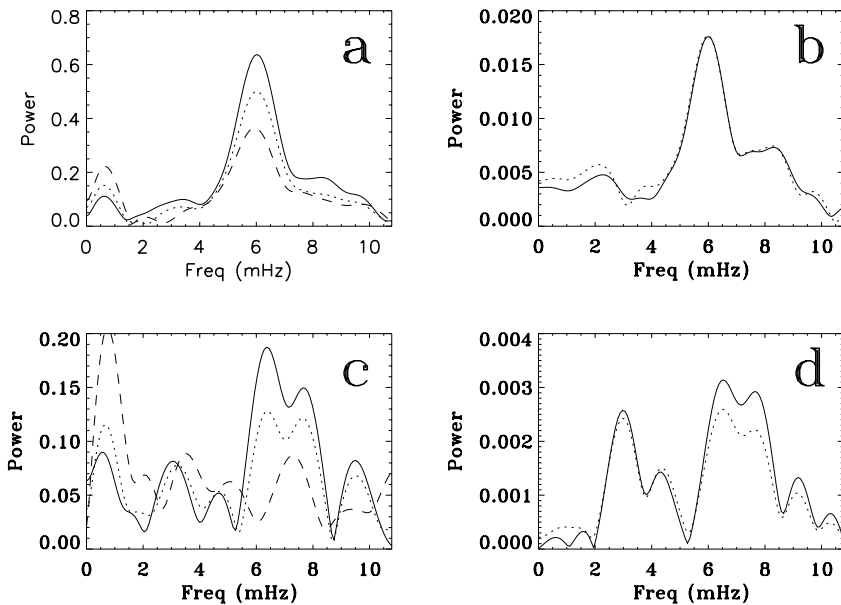


**Fig. 12.** **a)** Power spectra of the processed (see text) average intensity at line center (solid line),  $\pm 0.12$  Å (dotted line) and  $\pm 0.24$  Å (dashed line) of the umbral flash region. **b)** Power spectra of the processed average Doppler shifts at  $\pm 0.12$  Å (solid line) and  $\pm 0.24$  Å (dotted line) of the umbral flash region. **c)** Intensity power spectra figure for the dark umbra and **d)** Doppler shift power spectra figure for the dark umbra.

which could explain the observed change in the propagation of waves.

In Fig. 14 we show the maximum power frequency with distance from the center of the sunspot for the four different cuts that we have so far considered. It shows that the dominating frequencies in the umbra are near 6 mHz (167 s) and in the penumbra near 3 mHz (330 s). There is an abrupt decrease of frequency near the umbra – penumbra boundary and then the frequency remains almost constant in the penumbra where running penumbral waves dominate. However, in the outer penumbra there is again an abrupt decrease in frequency which may be due to the penumbra – superpenumbra boundary and a mixing of chromospheric oscillations and running penumbral waves. We also notice in the  $135^\circ$  cut that we find no frequency associated with penumbral waves for the lower right region of the sunspot, where the bright structure (BS) is observed.

## 5. Discussion and conclusions

Although the study of periodic phenomena like umbral flashes and RP waves in sunspots is important for the understanding of their structure, the physical mechanisms involved and the energy transported from them to their surroundings, no generally accepted model exists and their driving mechanism is still unknown. The determination of their different properties from observations in different spectral lines can help to test future theoretical interpretations.

Our umbral flash observations showed that they are localized phenomena. However it does not necessarily mean that they represent flux tubes of concentrated magnetic field embedded in a weaker umbral magnetic field. It could well be that umbral flashes are phenomena originating in small structures in the photospheric or the sub-chromospheric level and then channeled upwards through

a narrow path by the magnetic field hence preserving their original localized nature. It has been suggested that umbral flashes are the result of non-linear shock waves propagating upwards (López Ariste et al. 2001; Furusawa & Sakai 2000) or that their driving force is trapped magneto-acoustic waves in the photosphere (Thomas & Scheuer 1982) or in the chromosphere itself (Zhugzhda et al. 1985). A physical explanation is however beyond the scope of this paper, since a more detailed analysis of the relationship between umbral flashes and the magnetic field vector should be first performed.

Our study implies that the running waves originate inside the umbra since penumbral waves can be traced inside the umbra, as the power analysis shows. On the other hand, the time slice images of Fig. 11 give the impression that some oscillations in the umbra propagate outwards in the penumbra, although this is not always the case. There are umbral waves, e.g., that seem to fade away near the umbra-penumbra boundary probably because they do not have enough energy to sustain their propagation through the penumbra. The continuity of oscillations across the umbra-penumbra boundary reinforces earlier findings that there must be a connection between umbral oscillations and penumbral waves. The power analysis gives a frequency for running waves about half that of umbral flashes. This difference (which looks like a harmonic) could be attributed to a change of physical properties with distance from the center of the sunspot. However, no definite answer for the relationship between umbral flashes and RP waves could be given, as an indisputable physical model which could attribute these two phenomena to the same driving mechanism and also explain their differences is not available.

We found that the propagation velocity of penumbral waves as they move outwards decreases, in accordance with the results of Tsiropoula et al. (2000) for the H $\alpha$  line. Their average propagation velocity is larger than the

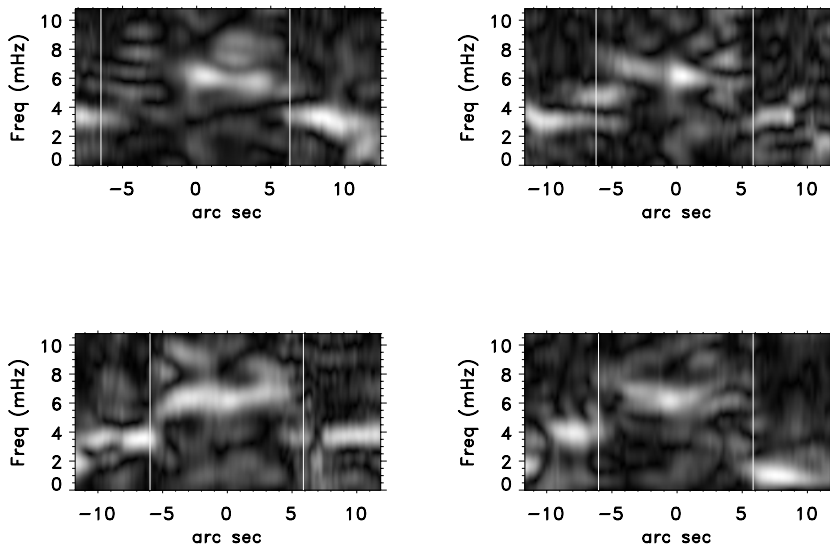


**Fig. 13.** The power amplitude of the spectrum analysis of Doppler shifts at  $\pm 0.12$  Å as a function of position from the center of the sunspot and frequency for the four cuts used in Fig. 11. The bright vertical lines mark the approximate boundary of the umbra.

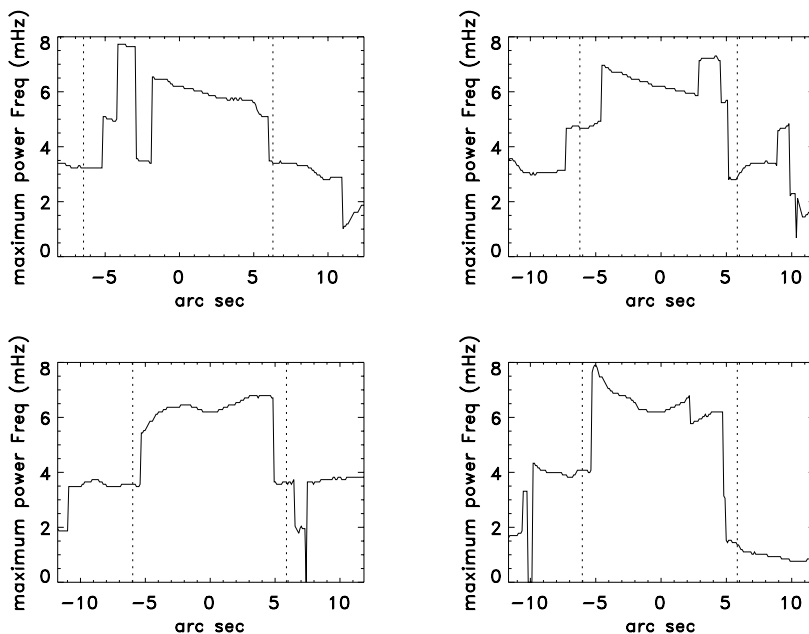


**Fig. 14.** The maximum power frequency as a function of position from the sunspot center for the four cuts used in Fig. 11. The dotted vertical lines mark the approximate boundary of the umbra.

sound speed in the atmosphere but much less than the chromospheric Alfvén velocity. This could be again attributed to different physical conditions or changes of the strength and inclination of the magnetic field with distance. Zhugzhda & Dzhililov (1984) have proposed the reverse inflowing Evershed flow as an explanation for the decrease in propagation velocity of running penumbral waves since they have to propagate against the flow.

It is obvious that the correlation of Doppler shifts of umbral flashes and running penumbral waves with the magnetic field vector is crucial in understanding their nature. Unfortunately the computed longitudinal magnetic field from the Stokes parameter  $V$  of the Ca II line is too noisy and no useful information could be extracted. Future observations should concentrate on high temporal and spatial spectropolarimetry measurements in multiple

lines. This would permit a detailed magnetic tomography of the sunspot region and lead to a better understanding of the nature of sunspot oscillations.

Moreover, detailed radiative transfer calculations of Ca II 8542 Å sunspot models are needed for the exact computation of the line-of-sight velocity during umbral flashes, when an emission appears on the blue side of the profile, permitting a better understanding of the dynamics of umbral oscillations.

*Acknowledgements.* We would like to thank all the THEMIS team and especially C. Briand for the efficient help during the observing campaign. This research is part of “Programme d’Actions Intégrées Franco-helléniques PLATON 2001” and the European Solar Magnetometry Network supported by the EC through the TMR programme.

## References

- Abdelatif, T. E., Lites, B. W., & Thomas, J. H. 1986, *ApJ*, 311, 1015
- Alissandrakis, C. E., Georgakilas, A. A., & Dialetis, D. 1992, *Solar Phys.*, 138, 93
- Alissandrakis, C. E., Tsiropoula, G., & Mein, P. 1998, in *ASP Conf. Ser. 155, Three-Dimensional Structure of Solar Active Regions*, ed. C. E. Alissandrakis, & B. Schmieder, 49
- Beckers, J. M., & Tallant, P. E. 1969, *Solar Phys.*, 7, 351
- Beckers, J. M., & Schultz, R. B. 1972, *Solar Phys.*, 27, 61
- Bhatnagar, A., Livingston, W. C., & Harvey, J. W. 1972, *Solar Phys.*, 27, 80
- Brisken, W. F., & Zirin, H. 1997, *ApJ*, 478, 814
- Brynildsen, N., Maltby, P., Leifsen, T., Kjeldseth-Moe, O., & Wilhelm, K. 1999, *Solar Phys.*, 191, 129
- Christopoulou, E. B., Georgakilas, A. A., & Koutchmy, S. 2000, *A&A*, 354, 305
- Furusawa, K., & Sakai, J. 2000, *ApJ*, 540, 1156
- Giovanelli, R. G. 1972, *Solar Phys.*, 27, 71
- Kneer, F., Mattig, W., & Uexküll, M. v. 1981, *A&A*, 102, 147
- Lites, B. W. 1986, *ApJ*, 301, 992
- Lites, B. W. 1992, in *NATO ASIC Proc. 375, Sunspots: Theory and Observations*, ed. J. H. Thomas, & N. O. Weiss (Kluwer Academic, Dordrecht), 261
- López Ariste, A., Socas-Navarro, H., & Molodij, G. 2001, *ApJ*, 552, 871
- Mein, P. 1991, *A&A*, 248, 669
- Mein, P. 1995, in *ASP Conf. Ser. 71, IAU Colloq. 149: Tridimensional Optical Spectroscopic Methods in Astrophysics*, ed. G. Comte, & M. Marcellin, 350
- Mein, P. 2002, *A&A*, 381, 271
- Semel, M. 1980, *A&A*, 91, 396
- Socas-Navarro, H., Trujillo Bueno, J., & Ruiz Cobo, B. 2000a, *Science*, 288, 1398
- Socas-Navarro, H., Trujillo Bueno, J., & Ruiz Cobo, B. 2000b, *ApJ*, 544, 1141
- Staude, J. 1998, in *ASP Conf. Ser. 184, Third Advances in Solar Physics Euroconference: magnetic fields and oscillations*, ed. B. Schmieder, A. Hofmann, & J. Staude, 113
- Thomas, J. H., & Scheuer, M. A. 1982, *Solar Phys.*, 79, 19
- del Toro Iniesta, J. C. 2001, in *ASP Conf. Ser., Magnetic fields across the Hertzsprung-Russell diagram*, ed. G. Mathys, & S. K. Solanki, in press
- Tsiropoula, G., Alissandrakis, C. E., & Dialetis, D. 1996, *Solar Phys.*, 167, 79
- Tsiropoula, G., Alissandrakis, C. E., & Mein, P. 2000, *A&A*, 355, 375
- Uexküll, M. v., Kneer, F., & Mattig, W. 1983, *A&A*, 123, 263
- Zhugzhda, Y. D., & Dzhililov, N. S. 1984, *A&A*, 133, 333
- Zhugzhda, Y. D., Locans, V., & Staude, J. 1985, *A&A*, 143, 201
- Zirin, H., & Stein, A. 1972, *ApJL*, 178, 85